PERGAMON

Quaternary Science Reviews 22 (2003) 659–671

QSR

Coupling of the hemispheres in observations and simulations of glacial climate change

A. Schmittner[a,*], O.A. Saenko[b], A.J. Weaver[b]

[a] *Max-Planck-Institut für Biogeochemie, P.O. Box 10 01 64, D-07701 Jena, Germany*

[b] *School of Earth and Ocean Sciences, University of Victoria, P.O. Box 3055, Stn CSC, Victoria, BC, Canada, V8W 3P6*

Received 26 June 2002; accepted 9 September 2002

Abstract

We combine reconstructions, climate model simulations and a conceptual model of glacial climate change on millennial time scales to examine the relation between the high latitudes of both hemispheres. A lead-lag analysis of synchronised proxy records indicates that temperature changes in Greenland preceded changes of the opposite sign in Antarctica by 400–500 yr. A composite record of the Dansgaard–Oeschger events shows that rapid warming (cooling) in Greenland was followed by a slow cooling (warming) phase in Antarctica. The amplitudes, rates of change and time lag of the interhemispheric temperature changes found in the reconstructions are in excellent agreement with climate model simulations in which the formation of North Atlantic Deep Water is perturbed. The simulated time lag between high northern and southern latitudes is mainly determined by the slow meridional propagation of the signal in the Southern Ocean. Our climate model simulations also show that increased deep water formation in the North Atlantic leads to a reduction of the Antarctic Circumpolar Current through diminishing meridional density gradients in the Southern Ocean. We construct a simple conceptual model of interhemispheric Dansgaard–Oeschger oscillations. This model explains major features of the recorded temperature changes in Antarctica as well as the general shape of the north–south phase relation found in the observations including a broad peak of positive correlations for a lead of Antarctica over Greenland by 1000–2000 yr. The existence of this peak is due to the regularity of the oscillations and does not imply a southern hemisphere trigger mechanism, contrary to previous suggestions. Our findings thus further emphasise the role of the thermohaline circulation in millennial scale climate variability.

1. Introduction

Recent synchronisation of records from the Greenland and Antarctic ice sheets has revealed that temperatures changed out of phase in both hemispheres during much of the last glacial period (Blunier et al., 1998). A process leading to such anti-phase behaviour is the thermohaline circulation (THC). Temperature changes in the northern and southern hemispheres are expected to be of opposite sign if the amount of North Atlantic Deep Water (NADW) is varied (Crowley, 1992; Stocker et al., 1992). This view is corroborated by observations (Hastenrath 1982; Hsiung, 1985) and ocean models (Bryan, 1986; Manabe and Stouffer, 1988; Maier-Reimer et al., 1990) which suggest that the heat flux in the Atlantic due to the THC is northward at all latitudes. Thus, a disruption of the circulation would lead to cooling in the northern hemisphere and warming in the southern hemisphere. Crowley's interhemispheric temperature seesaw has since served to identify and differentiate changes of the THC from other possible causes of recorded climate change (Stocker, 2000; Clark, et al., 2002).

However, important questions remain unanswered. Different authors (Bender et al., 1994; Charles et al., 1996; Blunier et al., 1998) report that temperature changes in Antarctica lead changes of the same sign in Greenland by 1000–2000 yr. A mechanism through which temperature changes could be transferred from Antarctica to Greenland with this time lag, however, is unknown. Such a lag is also apparently in contradiction to the paradigm that millennial scale variability is

*Corresponding author. Tel.: +49-3641-57-6273; fax: +49-3641-57-7200.

E-mail address: andreas.schmittner@bgc-jena.mpg.de (A. Schmittner).

URL: http://www.bgc.mpg.de/~andreas.schmittner.

0277-3791/03/$ - see front matter © 2002 Elsevier Science Ltd. All rights reserved.
PII: S0277-3791(02)00184-1

caused by changes in NADW (Charles et al., 1996). More detailed analysis of the phasing between the hemispheres has only recently been undertaken (Hinnov et al., 2002; Steig and Alley, 2002). Steig and Alley (2002) show that the phasing depends on the time scale of interest. For orbital variations Antarctica leads Greenland by 1000–1600 yr, while for higher frequency oscillations an additional peak occurs for Greenland leading Antarctica by 400–800 yr. They conclude that from the observations alone neither the "seesaw" theory (northern hemisphere trigger) nor the "southern lead" model can be supported. Hinnov et al. (2002), on the other hand, find West Antarctica (Byrd) leading Greenland by 400 yr in the "DO band" and another lead of Byrd by 1200 yr in a lower frequency band (0.2 cycles/kyr). They note, however, that these time leads are inconsistent and conclude that "the actual northern–southern relationship ... is most probably a simple antiphase". One purpose of the present study is therefore to reexamine the phasing in the proxy record and to investigate consistency with climate model simulations.

Important questions remain also unexplained in modelling interhemispheric climate change. One of the most robust features of climate model simulations forced with changes in the Atlantic THC is an antiphasing of subtropical South Atlantic temperatures with temperatures in the North Atlantic (e.g. Manabe and Stouffer, 1988; Mikolajewicz, 1996; Schiller et al., 1997; Rind et al., 2001). The response at high southern latitudes, however, is not unanimous. Some simulations show an antiphasing with the North Atlantic (e.g. Manabe and Stouffer, 1988; Schiller et al., 1997; Vellinga et al., 2002) while others predict an in-phase response (Manabe and Stouffer, 1997; Rind et al., 2001). Detailed analyses of the model simulations are rare and the processes through which the temperature signal is transmitted to high southern latitudes are virtually unexplored (with the exception of the study by Rind et al. (2001), who show a fast, in-phase response at high southern latitudes transmitted through the atmosphere). Therefore, another purpose of the present paper will be to fill this void.

In the reminder of the paper, we will examine the time lag between Greenland and West Antarctica in the proxy record (Section 2) as well as in simulations with a climate model (Section 3). We will then use the simulations to study the physical processes that determine the phasing between the hemispheres. In Section 4 we introduce a conceptual model of interhemispheric climate change in order to address the question concerning the location of the trigger mechanism.

Broecker (1998) proposed a bipolar seesaw in which the rate of deep water forming in the Southern Ocean would vary oppositely to that in the North Atlantic. This represents a different mechanism for interhemispheric teleconnections from the temperature seesaw described above and will not be the subject of the present paper.

2. The proxy record

We use the synchronised measurements of $\delta^{18}O$ from Greenland and West Antarctica from Blunier and Brook (2001) as shown in the upper panels in Fig. 1. In order to isolate millennial scale variability from variability on longer (Milankovich) time scales we re-sample the original data on a 10-yr interval and apply a triangular high pass filter with different length in a manner similar to that described in Alley et al. (2001). A time series with a 7000-yr cutoff frequency is shown in the lower panels of Fig. 1. The lead-lag analysis (Fig. 2) of the high pass filtered data suggests that Greenland leads West Antarctica by about 450 yr and the correlation for this time lag is negative. This means that warm phases in Greenland are followed by cold phases in West Antarctica and vice versa. A second extremum with positive correlation is present if the southern hemisphere leads the northern hemisphere by 1300 yr. Note that this maximum coincides with the maximum in the unfiltered data and is reminiscent of that found in south Atlantic deep sea sediments (Charles et al., 1996). We will address the question as to whether this maximum suggests a southern hemisphere trigger for interhemispheric climate change when we discuss results from the climate model (Section 3) and from the conceptual model (Section 4). Sensitivity tests with different cutoff frequencies showed that the results of the lead-lag analysis do not depend on the filtering of the data unless the length of the filter is shorter than about 5000 yr. The above results are consistent with the recent study by Steig and Alley (2002).

The syncronisation of the $\delta^{18}O$ from Greenland and West Antarctica is subject to uncertainty due to errors in the syncronisation of the methane gas records and due to errors in the differences between the age of the ice and the age of the enclosed gas bubbles. For the younger part of the records until 50 kyr (Dansgaard–Oeschger events 1–12) the total error has been estimated to be ± 300 yr (Blunier, personal communication). For some of the older events the error increases to ± 500 yr for DOs 14 and 16, to ± 650 yr for DOs 19–20 and to ± 750 yr for DO 21. Hence, the phase lag of 450 yr detected above is outside the error bars for the largest part of the records. The lag would not be affected by random errors in the syncronisation, e.g. if for some events the age had been overestimated and for others underestimated. We note, however, that the lag would be affected by a systematic error in the syncronisation of the two records. If, for example, the gas age in the Byrd record would be systematically underestimated for the

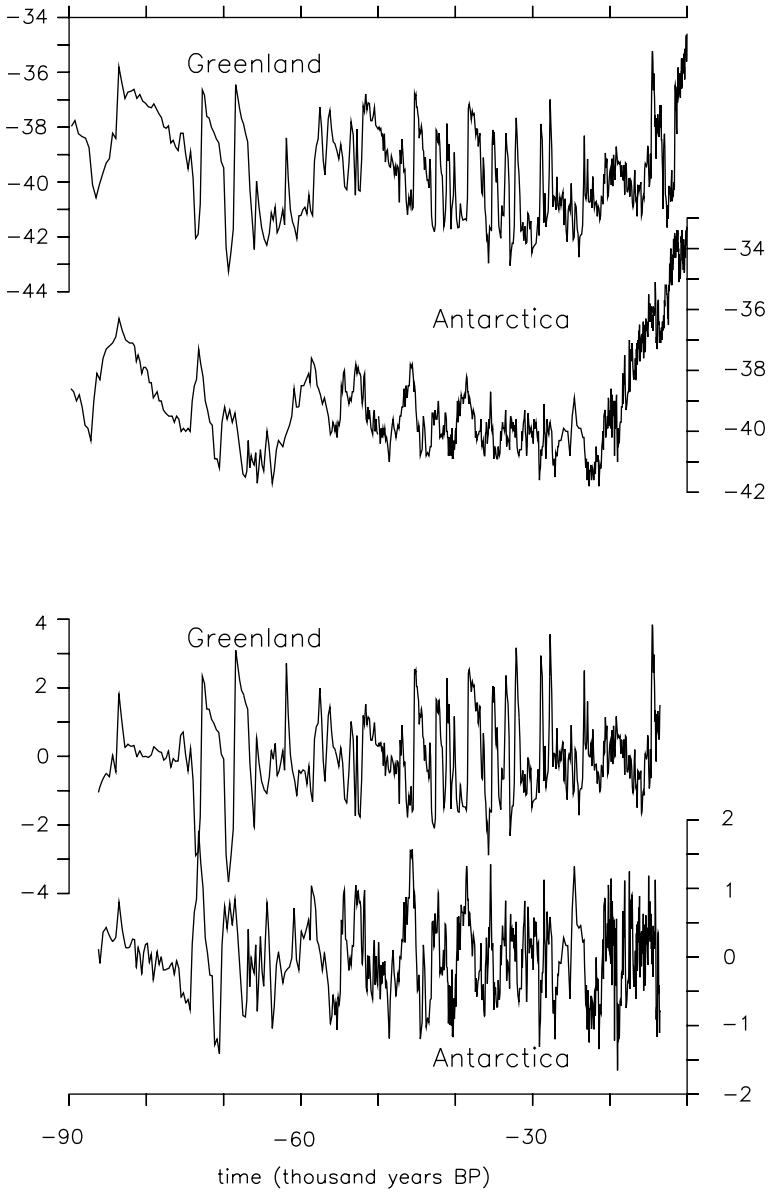

Fig. 1. $\delta^{18}O$ (in per mil) records from Antarctica and Greenland. Upper panels: original data from (Blunier and Brook, 2001). Lower panels: sampled and high pass filtered data.

entire time series then the lag with Greenland would be also be underestimated.

As the lead and lag analysis alone does not give us any information about the amplitude and rate of the temperature changes, we further calculate composites of Dansgaard–Oeschger (DO) events similar as in Schmittner et al. (2002). We synchronised the individual events around the times of rapid warming and cooling in Greenland (see Fig. 3). From the total of 21 DO events during the last glacial period we discarded DO 1 (Younger Dryas) because it occurs during the deglaciation and events 9, 13, 15, 16, 17 and 21 for the warming composite and events 2, 14, 15 and 16 for the cooling composite because they show no significant rapid change of state in the Greenland record, which makes it difficult to syncronise. In order to test the sensitivity of the results to this selection we also calculated the composite for all 21 events. This test (not shown) revealed that the composites do not depend on our selection of the DO events. However, the scatter in Fig. 3 increases somewhat if all 21 events are considered.

The composites together with the individual events shown in Fig. 3 suggest that the rapid warming in Greenland of $6\pm3^{\circ}C$ was followed by a slow cooling phase in West Antarctica during which temperatures decreased by about $1^{\circ}C$ within 500 yr. Cooling events of 3–$5^{\circ}C$ in Greenland are accompanied by a gradual warming of West Antarctica by less than a $1^{\circ}C$. From

the scatter in Fig. 3 we can also estimate the significance of the changes in the Antarctic record. The cooling trend can only be detected within an 80% confidence interval and the warming trend is even less significant. However, an in-phase response in West Antarctica can be excluded from Fig. 3. The amplitudes reported here are subject to uncertainties in $\alpha = \Delta T/\Delta\delta^{18}O$ (see Jouzel et al., 1997 for a review). For Greenland, values vary between $\alpha = 3^{\circ}C$/mil for estimates based on borehole measurements (Cuffey et al., 1995) and today's spatial relation of $\alpha = 1.5^{\circ}C$ per mil (Johnsen et al., 1989). The value we use here (1.85°C per mil) is based on nitrogen and argon isotope measurements of the warming event DO 12 (Caillon et al., 2001). For Antarctica, a similar large range of estimates exist from $\alpha = 1^{\circ}C$ per mil to 2°C per mil (see also Section 5).

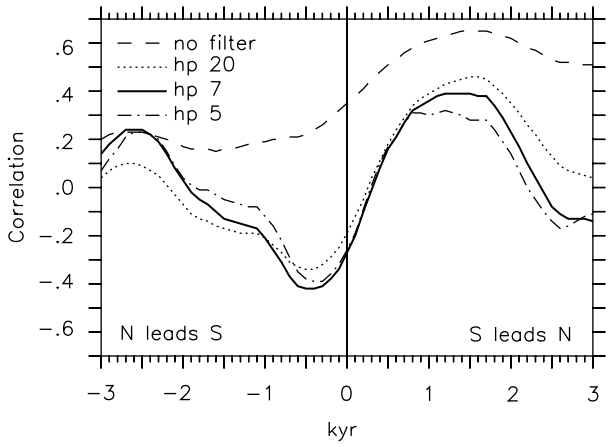

Fig. 2. Cross correlation between Greenland and Antarctic temperatures as function of the lag between both timeseries. Negative values for the lag indicate that the northern (N) hemisphere leads the south (S) and vice versa. High pass filters with different cutoff frequencies are applied to the original data from (Blunier and Brook, 2001). Dashed line: no filter, dotted line: 20 kyr cutoff frequency, solid line: 7 kyr, dash–dotted line: 5 kyr cutoff frequency. The unfiltered data show a single maximum around 1500 yr, while the high pass filtered data all show a second extremum with negative correlation between −300 and −500 yr.

3. Climate model simulations

3.1. Model description

For the simulations we employ a model of the glacial ocean–atmosphere–sea ice system similar to that used by Schmittner et al. (2002), which is described in detail in Weaver et al. (2001). This model comprises an ocean primitive equation general circulation model (Pacanowski, 1995), a vertically integrated energy–moisture balance model of the atmosphere based on Fanning and Weaver (1996) and a dynamic–thermodynamic sea ice model (Bitz et al., 2001). The differences from Schmittner et al. (2002) involve computation now on a rotated grid, prescribed continental ice sheets after Peltier (1994)

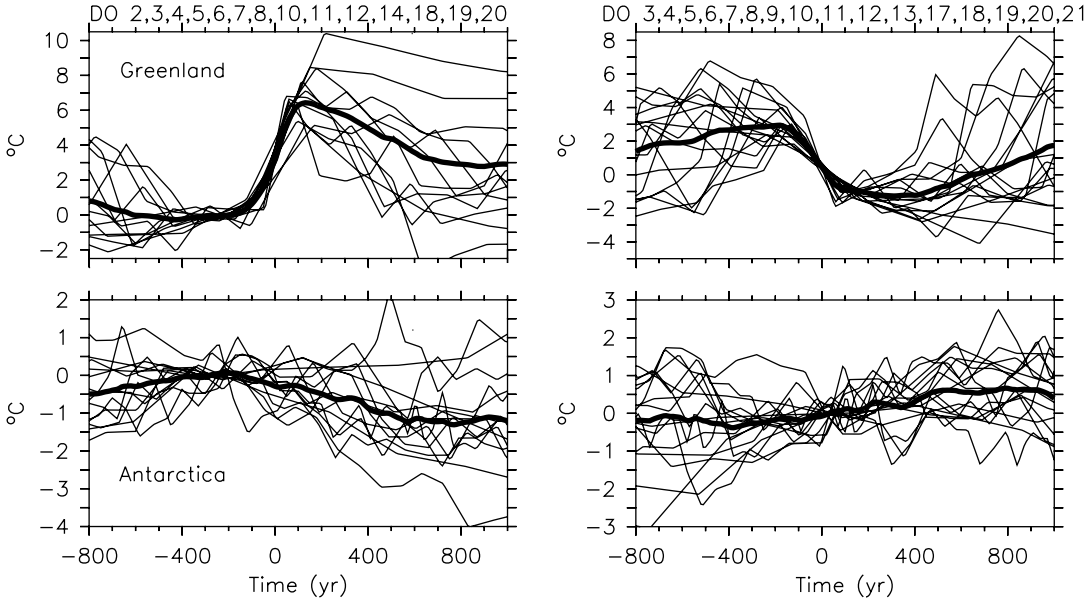

Fig. 3. Reconstructed surface air temperatures in the northern (upper panels) and southern (lower panels) hemisphere for individual DO events (thin lines) and their composite (thick lines). Left panels: warming events. Right panels: cooling events. We assume a linear relation between changes in the oxygen isotope ratio $\Delta\delta^{18}O$ and surface air temperature ΔT according to $\Delta T = \alpha\Delta\delta^{18}O$. For Greenland $\alpha = 1.85^{\circ}C$ per mil (Caillon et al., 2001) and for Antarctica $\alpha = 1.5^{\circ}C$ per mil (Salamatin et al., 1998) was chosen. The individual records are horizontally shifted such that the warming/cooling events in Greenland occur near year 0 and vertically shifted such that the time mean between year −400 and −100 for the warming events and between years −100 and 200 for the cooling events is zero.

and the use of isopycnal mixing in the ocean model together with a parameterisation of mesoscale eddy activity (Gent and McWilliams, 1990), as well as advection of specific humidity in the atmosphere. Present day wind velocities are prescribed for the moisture advection and momentum transfer to the ocean and sea ice. We show results from two experiments which differ only in the wind stress forcing of the Southern Ocean. In the standard experiment, wind stress is applied to the ocean whereas in experiment W we set wind stress to zero over the ice free ocean south of 30°S in order to reduce the Antarctic Circumpolar Current (ACC).

3.2. Results

We force the model with linearly increasing or decreasing (at a rate of 0.6 Sv/1000 yr) freshwater input into the North Atlantic (see top panel in Fig. 4) as in Schmittner et al. (2002). This forcing function was not designed in order to achieve agreement with the observations, but rather was used to provide an idealised perturbation to the system in order to trigger transitions between different states of the THC. Therefore, it is only necessary that the forcing exceeds a certain threshold value. The functional form is of secondary importance and could have also been different (e.g. a sinusoidal).

In the standard experiment, the North Atlantic overturning is initially in a weak stadial state (4 Sv) but between model years 500 and 600 it exhibits a rapid transition to an interstadial state with more than 20 Sv of deep water formation. After year 700, the overturning declines almost linearly for about 800 yr. Note that despite the symmetric forcing the model response is asymmetric. Modelled air temperatures in Greenland also show an asymmetric sawtooth-shaped evolution. An abrupt warming of about 5°C for the transition from the stadial to the interstadial state (Fig. 4) is followed by a gradual temperature decrease until around year 1000, when a rapid cooling of more than 2°C terminates the interstadial state. This abrupt cooling is associated with a collapse of convection in the Labrador Sea (not shown). The amplitude and rate of the rapid warming, the sawtooth-shaped evolution of the interstadial, and the rapid cooling event at the termination of the interstadial are in excellent agreement with the composite proxy record. Antarctic temperatures show a gradual cooling after the transition to the interstadial state. The maximum cooling of 0.8°C is reached approximately 400 yr after the maximum warming in Greenland. The modelled rate of the cooling as well as the amplitude are in excellent agreement with the reconstructed composite.

A similar time lag of 300–400 yr between Antarctica and Greenland also appears in the lead-lag analysis of

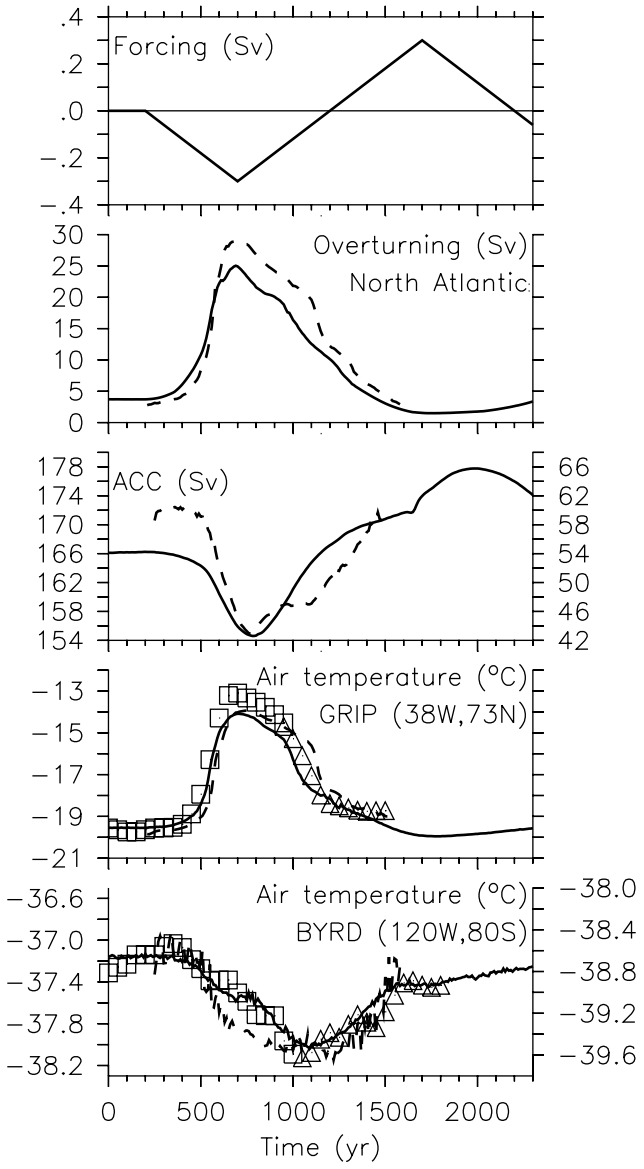

Fig. 4. Climate model simulations. Time series from two experiments are shown. Solid lines: standard experiment. Dashed lines: experiment W in which wind forcing of the surface ocean south of 30°S is suppressed. Top panel: fresh water forcing in the North Atlantic. Second panel: overturning in the North Atlantic. Third panel: flow though Drake Passage. Left axis: standard experiment. Right axis: experiment W. Forth panel: Greenland surface temperature. Bottom panel: Antarctic surface temperature. Left axis: standard experiment. Right axis: experiment W. Square (triangle) symbols in the lower two panels denote the composites of the reconstructions synchronised around the warming (cooling) events as given in Fig. 3. The composites have been shifted horizontally such that the rapid warming (cooling) event in Greenland occurs at the same time as in the simulation and vertically such that the mean values before the rapid warming are roughly equal to the simulated values.

the standard model simulation (Fig. 5). This is close to the 450-yr time lag found in the proxy record (Fig. 2). Encouraged by this agreement we want to analyse the propagation of the signal in the simulations in order to

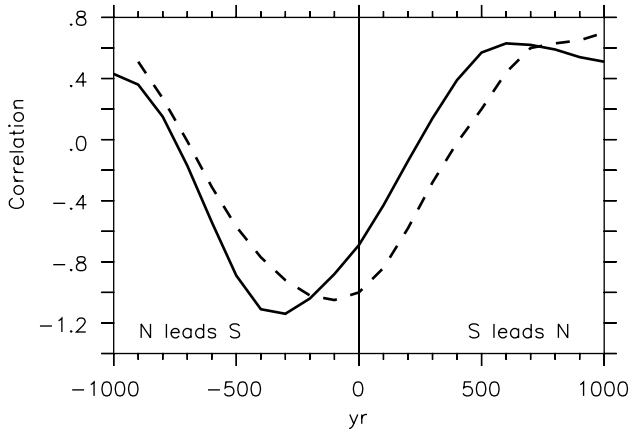

Fig. 5. As in Fig. 2 but for the simulations. Solid lines: standard experiment. Dashed lines: experiment W (see Fig. 4). Due to the short time series only lags between −1000 and +1000 yr are shown. For the standard experiment large negative correlation coefficients of $r < -0.9$ are found if Greenland leads Antarctica by 300–400 yr. For experiment W this lead is with 100 yr much shorter. Note that the absolute values of the correlation coefficients are much larger for the simulation than in the reconstructions since the model does not exhibit internal variability.

understand the processes which determine the time lag. In Fig. 6 we show the propagation of the signal in the South Atlantic. The signal appears first at subsurface depths with a time lag of only 40 yr relative to the North Atlantic. This time lag is in good agreement with the recent study by Johnson and Marshall (2002), who show that the adjustment of the upper ocean is determined by fast Kelvin waves propagating along the boundaries and the equator and subsequent radiation of Rossby waves into the interior. At the surface the time lag is somewhat longer (70 yr), which is likely due to the attenuation of the surface signal by the atmosphere. The cooling appears almost simultaneously between 20°S and 40°S. Its further southward propagation, however, is delayed. At the surface the signal reaches 60°S about 400 yr after the warming in the North Atlantic and at greater depth this time lag is even larger. The slow southward propagation between 40°S and 60°S is due to the presence of the ACC at those latitudes. This is illustrated by the results of experiment W in which the Southern Ocean is not driven by winds. In this experiment, the ACC has only 1/3 the strength of that in the standard experiment (see Fig. 4 third panel), leading to a faster meridional propagation of the temperature signal in the Southern Ocean (dashed lines in Fig. 6) and hence a much shorter time lag of Antarctic air temperatures with those in Greenland (Fig. 5). Thus, the comparison of our two experiments indicates that the time lag of high latitude air temperatures is mainly determined by the strength of the ACC. This is consistent with the finding that high latitude waters are isolated from lower latitudes both dynamically and thermally due to the existence of the ACC (Cox, 1989).

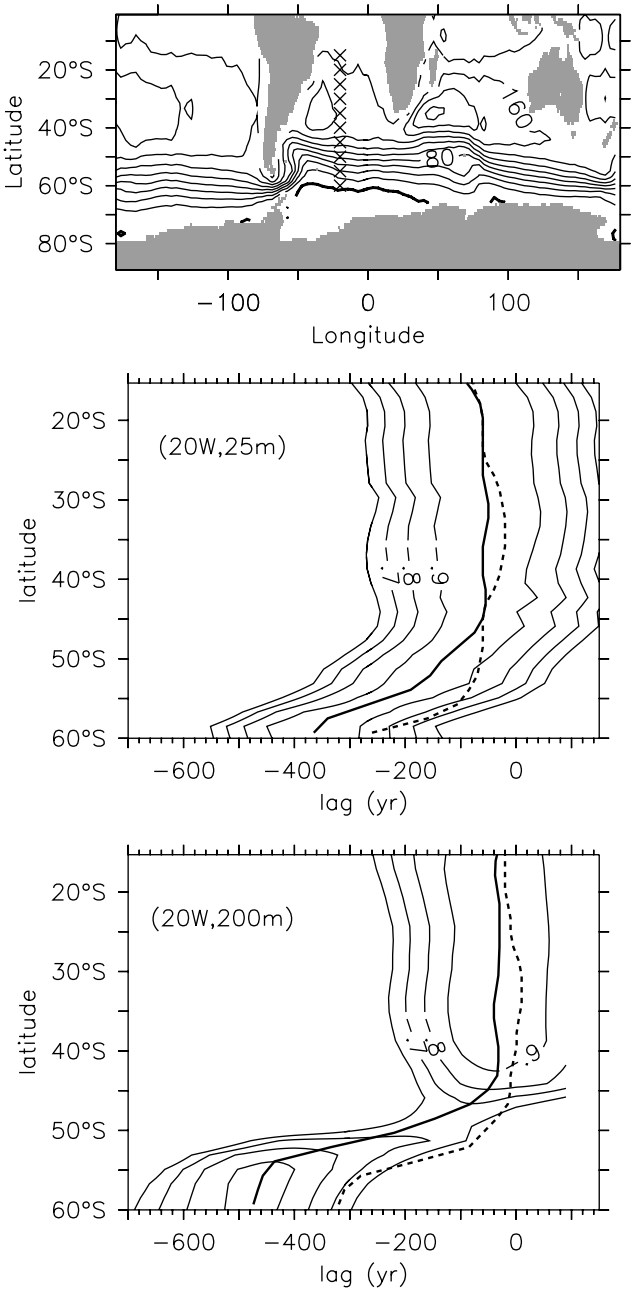

Fig. 6. Propagation of the temperature signal in the South Atlantic. Top panel: Antarctic Circumpolar Current (ACC) in the standard experiment at year 0. Isoline difference is 20 Sv. The crosses at 20°W indicate the section shown in the lower panels. Lower panels: Thin lines denote the cross correlation of potential temperature along the section at 20°W shown in the top panel with SST in the North Atlantic (30°W, 50°N) for the standard experiment. Middle panel: Propagation at the surface (25 m). Bottom panel: Propagation at subsurface levels (200 m). Negative values for the lag indicate that North Atlantic SSTs lead temperatures in the South Atlantic. The minimum correlation (thick lines) gives the time lag with North Atlantic SSTs for the standard experiment (solid) and experiment W (dashed).

A sensitivity experiment (not shown) with lateral instead of isopycnal mixing and without the parameterisation of eddy-induced tracer advection (Gent and

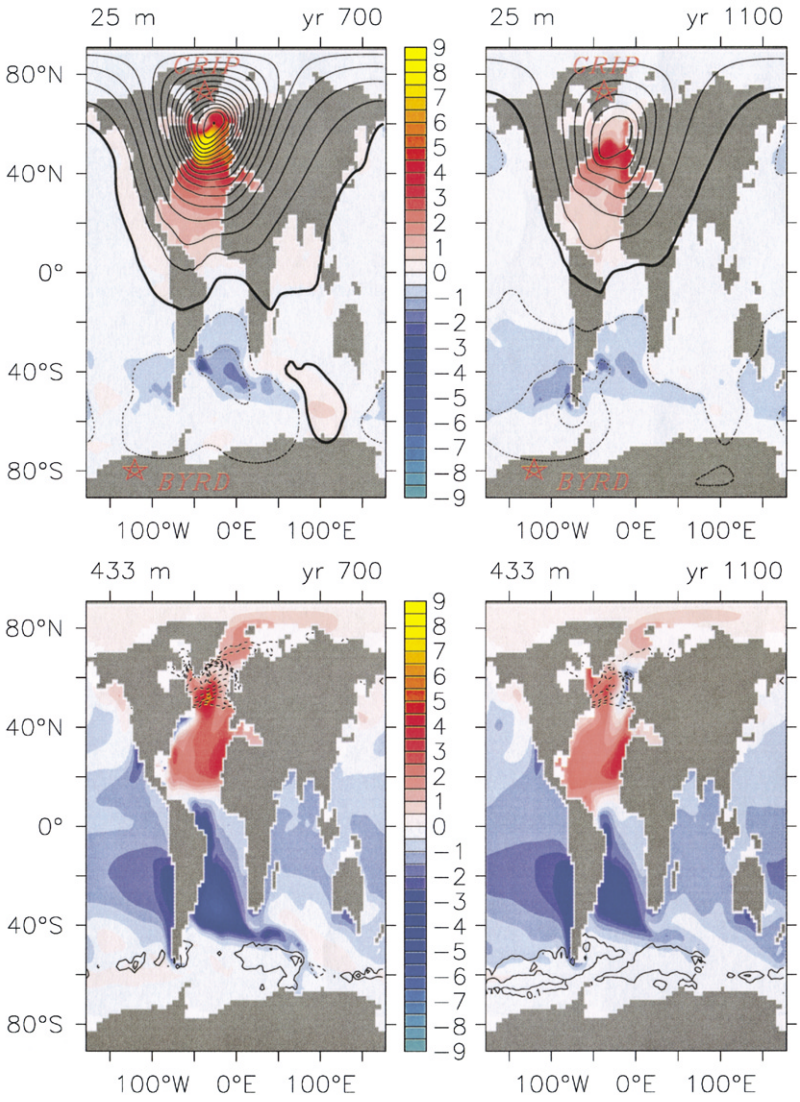

Fig. 7. Anomalies (differences from year 0) of different variables in the standard experiment. Colour contours: potential temperature at the sea surface (upper panels) and at 433 m depth (lower panels) at year 700 (left) and year 1100 (right). Line contours in upper panels: surface air temperature (0.5°C isoline differences, negative values dashed, zero line thick). Line contours in lower panels: sea ice concentration (isolines at ± 0.05, ± 0.15, etc.).

McWilliams, 1990) showed a significantly shorter time lag, suggesting that diffusive and advective processes play a role in the propagation of the signal through the Southern Ocean.

Around the time of maximum warming in Greenland (year 700), cooling of the air temperatures is largest over the South Atlantic around 40°S (Fig. 7). This pattern is strongly determined by the SST changes. Sea ice has increased over much of the Southern Ocean, particularly over the western Indian Ocean sector. The concentration of sea ice keeps increasing for the following four centuries, mainly in the Atlantic and Pacific sectors of the Southern Ocean. This slowly increasing sea ice cover amplifies the cooling of the high latitude atmosphere.

The temperature signal in the South Atlantic is largest (more than 5°C cooling at 433 m) at subsurface levels (Fig. 7) around 35°S. We suggest therefore that in the South Atlantic it might be advantageous to look for the signal in deeper dwelling species of foraminifera than at surface dwelling species.

Cooling of the upper water column in the southern hemisphere is more pronounced at lower latitudes. This decreases the meridional density gradient, which weakens the strength of the ACC (see Fig. 4). The flow through Drake Passage varies by about 20 Sv with reduced flow during the interstadial phase in which NADW formation is strong and maximum flow during the stadial phase around year 2000.

Rind et al. (2001) report an increase of the ACC by about 30 Sv for NADW reduction by 15 Sv. They attribute the increased ACC to stronger westerlies in their atmospheric model component. In our simulations, in which changes in atmospheric dynamics are absent, the ACC variations are purely thermohaline driven. Therefore, we suggest that a considerable part of the increased ACC reported by Rind et al. (2001) is also associated with buoyancy effects through the joint effect of baroclinicity and relief (JEBAR). However, the magnitude and rapidity of the changes in Rind et al. (2001) indicate that wind forcing also contributes to their simulated variations in the ACC. In agreement with the study of Rind et al. (2001) we find that the changes in the ACC lead to variations in ocean heat convergence in the Southern Ocean and hence cause the zonal asymmetries in the surface temperature and sea ice response seen in Fig. 7.

Generally, the model response at the surface (Fig. 7) is consistent with a recent compilation of reconstructions of millennial scale climate change during the last deglaciation (Clark et al., 2002). The spatial patterns revealed by their synthesis shows antiphasing between the North Atlantic and marine records from the South Atlantic and most terrestrial records from Antarctica. Records from the west coast of the Americas north of 20°S and one record from the Arabian Sea are in-phase with the North Atlantic. This pattern is in agreement with our model results. The only significant difference between the observations and our simulation is an SST record in the tropical Atlantic which shows antiphasing with North Atlantic proxies. This near-shore record might be significantly influenced by variations in wind-induced upwelling (Rühlemann et al., 1999), which are not captured in our model.

4. A conceptual model

In the previous sections, we have seen that the prominent peak in the lead-lag diagram of the observations, with changes over Greenland leading changes over West Antarctica by 400–500 yr (Fig. 2), is in good agreement with our standard climate model simulation (Fig. 5). This provides evidence for the notion that a large part of the interhemispheric temperature correlations observed during the last glacial period can be explained by perturbations of NADW. However, in the observations a second extremum is present, with Antarctica leading temperature changes of the same sign in Greenland by 1300 ± 500 yr (Fig. 2). Here, we address the question as to whether this peak can also be explained by a northern hemisphere trigger (“seesaw”) or whether we require an additional mechanism with a trigger in the southern hemisphere (“southern lead”). In the “southern lead” case, we were confronted with the problem of an unknown mechanism in the climate system, which would lead to temperature changes in Greenland 1300 yr after changes of the same sign in Antarctica. In the following, we will examine the “seesaw” case. If this examination provides a positive answer, then we will have circumvented the problem associated with the “southern lead” case.

We consider the following example, which illustrates one hypothetical way a peak around year 1300 in Fig. 2 could be produced by a northern hemisphere trigger mechanism. Assume a very regular forcing of period $T \simeq 3500$ yr in Greenland producing a very regular response of the opposite sign in Antarctica with a time lag of 450 yr. In this case, peaks of negative correlation at times $-450 \pm NT$ and positive peaks at times $-450 + (1/2 \pm N)T$ would occur, where $N = 0, 1, 2, 3, \ldots$ is a non-negative integer. Thus, for $N = 0$ we would get a positive peak at year 1300, thereby prompting the question as to whether the DO events occurred with a regular period of 3500 yr. During the 70 kyr record from 15 kyr BP to 85 kyr BP 20 DO oscillations occurred (see Fig. 1) yielding an average period of exactly 3500 yr! Indeed, initial tests using a stochastic resonance model (Alley et al., 2001) with that period showed that if the forcing was very regular, a prominent peak around 1300 yr occurred as in the reconstructions and as expected from the above thought experiment. However, the existence and magnitude of this peak was found to be highly sensitive to the regularity in the forcing. These initial tests and the appreciation of the correct regularity in the forcing (Greenland temperatures) led us to the following model in which we approximate the regularity of the forcing from the observations.

As the simplest model of DO oscillations in Greenland we assume two states: $T_G = -1$ represents the cold stadial states and $T_G = 1$ represents warm interstadials. Stepwise transitions between these two states occur at times specified from the observations and given in Table 1. Note that generally the times of the rapid warmings can be readily diagnosed from the record, while some of the cooling events cannot be timed exactly and uncertainties increase accordingly. As such, Greenland temperatures are prescribed in the model with approximately the correct spacing (regularity) between the events.

Motivated by the results of our composite analysis and the climate model simulations (see Figs. 3 and 4) we assume that Antarctic temperatures T_A respond to rapid warmings (coolings) in Greenland (T_G) with a linear cooling (warming) phase

$$\frac{\partial T_A}{\partial t} = -T_G s,$$

where $s = \Delta T_A / \Delta t$ is the slope, $\Delta T_A = T_A^{max} - T_A^{min} = 2$ is the difference between the warmest $T_A^{max} = 1$ and coldest $T_A^{min} = -1$ states in Antarctica and Δt is the time

Table 1
Times of rapid warming and cooling events used in the conceptual model in years BP on the GISP2 time scale as in Blunier and Brook (2001)

DO-event	Cooling	Warming
2	23250	23400
3	27450	27850
4	28600	29000
5	31600	32300
6	32970	33550
7	34450	35280
8	36200	38410
9	40000	40180
0	40650	41150
11	41580	42530
12	43130	45370
13	46410	47200
14	49000	52100
15	53100	53700
16	54500	56600
17	57300	58400
18	61600	62000
19	66700	68650
20	69800	72900
21	73800	83750

required for a transition between them (see upper panels of Fig. 8).

The only free parameter of the model is the slope s or equivalently Δt. Note that short events in Greenland cause a smaller response in Antarctica for large values of Δt. The reason is that an ongoing temperature trend in Antarctica can be interrupted by a state transition in Greenland. As an example, a high pass filtered model with $\Delta t = 1333$ yr is shown in Fig. 9 together with the observations. Prominent features of the Antarctic temperature variations during the last glacial period are reproduced by the simple model. These features include the major Antarctic warm events A1–A6 (Blunier and Brook, 2001) as well as several smaller warm events after A1 and between A1 and A2. The correlation between the simple model and the observations is 0.48, suggesting that the model explains a significant part (23%) of the observed variability in Antarctica.

We would expect that the choice of Δt also determines the time lag between Greenland and Antarctica. If Greenland temperatures would reside longer than Δt in each state, then the highest correlation would be obtained for T_G leading T_A by $\Delta t/2$. However, since many events in Greenland are shorter than Δt the average lead (as the location of the minimum correlation) depends only weakly on Δt (see Fig. 10). Generally, the shape of the interhemispheric phase relation in the model is in surprisingly good agreement with the observations (Fig. 10). Not only the negative correlations around −400 yr, but also the broad area of

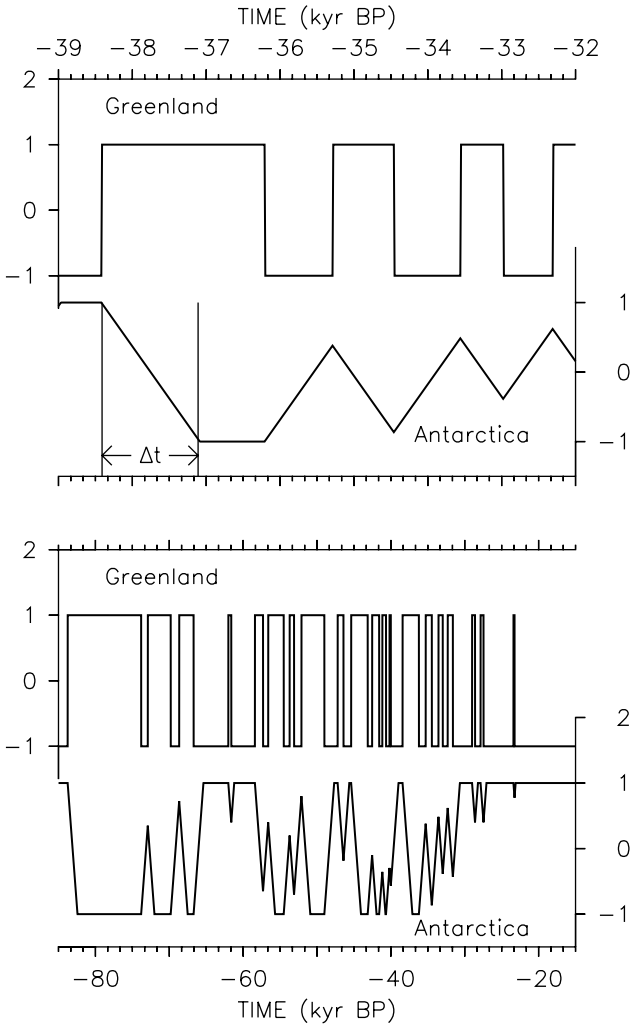

Fig. 8. Conceptual model of interhemispheric Dansgaard–Oeschger oscillations. Top panels: DO events 8, 7, 6 and 5 as examples of the model with $\Delta t = 1333$ yr. Antarctic temperatures respond with a linear transition of the opposite sign to stepwise changes in Greenland. Bottom panels: full time series for the model with $\Delta t = 1333$ yr.

positive correlations between 500 and 2000 yr, and a second area of positive values between −3000 and −2000 yr, are captured by the model. For very small values of Δt an additional maximum around −1300 yr appears and very large Δt lead to a pronounced maximum around 500 yr both of which are not present in the observations. Hence, we conclude an intermediate value of Δt between 800 and 1333 yr is in best agreement with the observations. This range of values for Δt is also consistent with our climate model simulations. Additional experiments with long interstadials (not shown) indicate values of more than 1100 yr for Δt.

The main differences between the model and the observations are too large values of the correlation around year −400 and too small values around year 1300. However, so far we did not consider noise, which is clearly present in the observations. In order, to

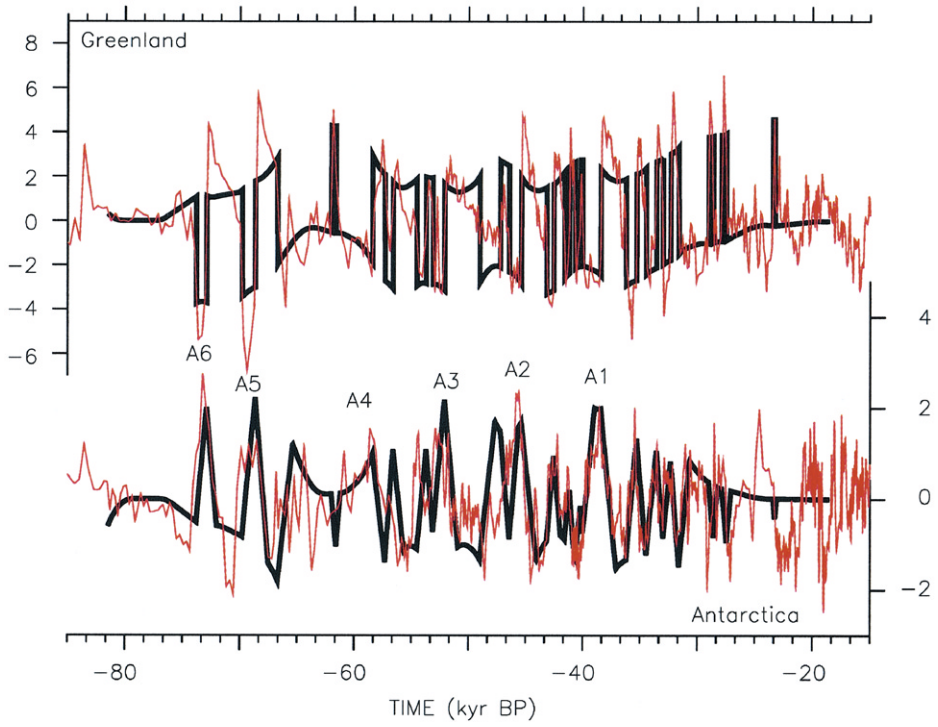

Fig. 9. High pass filtered (cutoff frequency at 7000 years) model temperatures (black lines, $\Delta t = 1333$ yr, see Fig. 8) together with the observations (red lines, from Fig. 1). Units are °C and the conversion from $\delta^{18}O$ to temperature for the observations has been done as explained in the caption of Fig. 3. Model temperatures are scaled by 2.4 (Greenland) and 1.7 (Antarctica) in order to fit the observations.

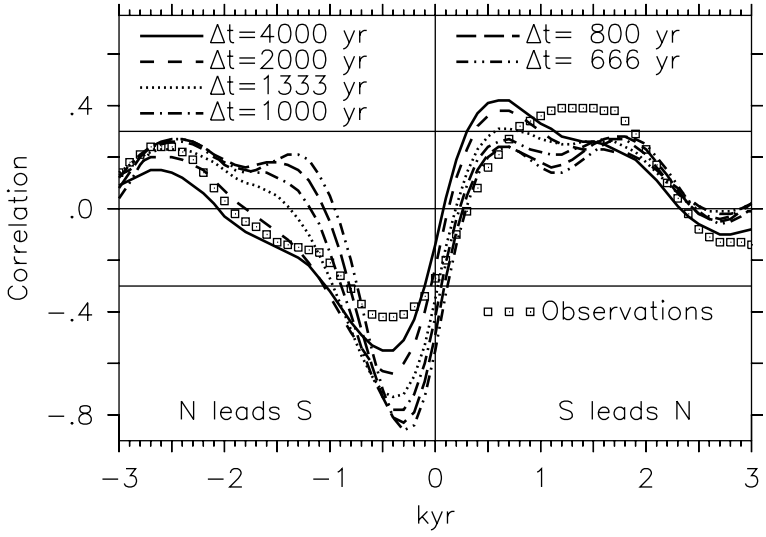

Fig. 10. As in Fig. 2 but for the conceptual model. The different lines correspond to different values of Δt. Square symbols give the observed phase relation from Fig. 2.

account for the effect of uncorrelated internal variability in the observations we produce 100 representations of red noise, which we add to the results of the deterministic model described above. In order to determine the signal-to-noise ratio we used the following approach. First, we scaled the results from the deterministic model such that the major events are of similar amplitude to the observations (Fig. 9). Next, we assume that the variance of the scaled model represents the variance of the signal σ_S^2 and the variance of the observations represent the total variance σ^2. Assuming the signal and noise are uncorrelated the variance of the noise is $\sigma_N^2 = \sigma^2 - \sigma_S^2$. This procedure gives signal-to-noise ratios σ_S/σ_N of approximately 2 for Greenland

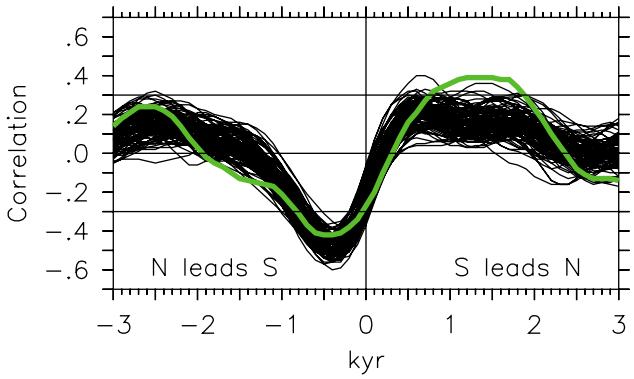

Fig. 11. As Fig. 10 but for a model ($\Delta t = 1333$ yr) including noise. Red noise with decorrelation times of 1–2 kyr was added to the deterministic model using signal to noise ratios of 2 for Greenland and 1.5 for Antarctica as estimated from Fig. 9. Different thin lines correspond to different representations of the noise. The observed phase relation is shown as the thick green line.

and 1.5 for Antarctica. Note, however, that the uncertainty in the estimation of the signal-to-noise ratios is large since it depends on the scaling factors.

Fig. 11 shows that for the stochastic model, the amplitude of the correlation around year −400 is reduced from values around −0.7 for the deterministic model (see Fig. 10) to values around −0.4, consistent with the observations. Generally, the observations are enclosed by the scatter of the stochastic model everywhere except near year 1300, where the observations slightly leave the envelope of the model. The fact that the large amplitude of the maximum around year 1300 cannot be explained by our simple model suggests that we cannot exclude a mechanism operating from the southern hemisphere. However, the similarity between the phase diagram of the model and that of the observations, including the broad positive peak around 1300 yr makes a strong case for a mechanism of DO oscillations involving a trigger in the North Atlantic and does not leave much room for alternative mechanisms such as the "southern lead" model.

5. Discussion

We have shown in Section 3 that the amplitude of the climate model response in Antarctica is in good agreement with the composite record of the DO events ($\simeq 1$°C, see Fig. 4). Some warming events in Antarctica (A1–A7), however, seem to show a stronger amplitude ($\simeq 2$°C, Indermühle et al., 2000), as also indicated by the scaling of the conceptual model (see Fig. 9). The reason of this discrepancy is not clear, although it might be related to: (1) uncertainties in the relation between δ^{18}O and air temperature and/or (2) missing feedbacks with the carbon cycle.

(1) From Salamatin et al. (1998) we infer the uncertainty for α to be about 1.5 ± 0.5 K per mil. Thus, the largest Antarctic δ^{18}O variations of about 1.5/mil would translate to 1.5–3°C temperature changes.

(2) Warming events A1–A7 in Antarctica all start during a cold phase in Greenland. We propose that a prolonged shutdown of NADW formation causes the observed increase of atmospheric CO_2 which accompanies these events (Indermühle, et al., 2000). This assumption is consistent with modelling exercises (Marchal et al., 1999). Increasing atmospheric CO_2 could then amplify the warming in Antarctica. 15 ppmv changes in atmospheric CO_2 could account for around 0.5°C warming and bring our modelled amplitude into the lower range of the observations. In order to test this hypothesis more quantitatively, we plan to extend our climate model simulations including a model of the ocean carbon cycle (Ewen et al., 2002).

While interpreting the results of our climate model simulation it must be kept in mind that the atmospheric model component is highly simplified. Feedbacks associated with changed atmospheric dynamics or cloud cover, albeit highly uncertain, are not included and could significantly change the model response. Therefore, it is desirable that similar simulations are repeated with fully coupled GCMs in which representations of these feedback mechanisms are included.

While we have demonstrated that the climate model used in the present study exhibits a bipolar seesaw of high latitude air temperatures in agreement with the observations, other model studies report differing results. Manabe and Stouffer (1997, 2000) and Rind et al. (2001) find warming in the subtropics of the southern hemisphere for a shutdown overturning. High southern latitudes in their coupled ocean–atmosphere GCMs, however, show a slight cooling. The coupled GCMs of Vellinga et al. (2002); Schiller et al. (1997) and Manabe and Stouffer (1988), on the other hand, produce an anti-phasing of the high latitudes similar to the present model as do other simplified models (e.g. Mikolajewicz, 1996; Ganopolski and Rahmstorf, 2001).

The bipolar temperature seesaw also remains controversial from the perspective of reconstructions. Observations from Taylor Dome at the western edge of the Ross Sea show synchronous temperature changes with Greenland during the last deglaciation (Steig et al., 1998) and thus seem to contradict the anti-phase theory. However, a syncronisation of the Taylor Dome record with the more inland Dome C ice core based on high-resolution calcium measurements has questioned this conclusion (Mulvaney et al., 2000). Also, we have

seen that considerable zonal asymmetries can arise in Southern Ocean SSTs and air temperatures in response to a collapsed overturning (Fig. 7), suggesting that the seesaw pattern might not be present everywhere in Antarctica.

6. Conclusions

Contrary to previous suggestions that Antarctica leads Greenland by 1000–2000 yr (Bender et al., 1994; Charles et al., 1996; Blunier et al., 1998) we have shown that the phase lag between the hemispheres on millennial time scales is such that Greenland leads changes of the opposite sign in Antarctica by 400–500 yr. The peak for a southern lead of 1000–2000 yr is a consequence of the regularity of the DO oscillations and does not imply a southern hemisphere trigger.

Experiments with a climate model indicate that the time lag of 400–500 yr is determined by the slow meridional propagation of the signal in the Southern Ocean across the latitudes of the ACC. Thus, the response at high southern latitudes is not synchronous with the north and the rate of change of high southern latitude temperatures is much slower than estimated earlier by simple thermodynamic considerations (Stocker, 1998). The reason for the slow propagation is related to the missing zonal boundaries around the latitudes of Drake Passage. This prohibits the propagation of fast boundary trapped waves and isolates high latitude waters effectively from latitudes further north (Cox, 1989).

The observed phasing between the hemispheres can almost entirely be explained with a model of Dansgaard–Oeschger oscillations based on perturbations of the Atlantic thermohaline circulation. This indicates that the main mechanism producing interhemispheric temperature correlations on millennial time scales during the last glacial period was very likely fluctuations in the rate of deep water formation in the North Atlantic.

Acknowledgements

Comments from R.B. Alley, an anonymous referee and the editor P.U. Clark were appreciated. This research was supported by grants from the Natural Sciences and Engineering Research Council of Canada, the Canada Research Chair Program, the Meteorological Service of Canada/Canadian Institute for Climate Studies (through the Canadian Climate Research Network), and the Canadian Foundation for Climate and Atmospheric Sciences.

References

Alley, R.B., Anandakrishnan, S., Jung, P., 2001. Stochastic resonance in the North Atlantic. Paleoceanography 16, 190–198.

Bender, M., Sowers, T., Dickson, M.-L., Orchardo, J., Grootes, P., Mayewski, P.A., Meese, D.A., 1994. Climate correlations between Greenland and Antarctica during the past 100,000 years. Nature 372, 663–666.

Bitz, C.M., Holland, M.M., Weaver, A.J., Eby, M., 2001. Simulating the ice-thickness distribution in a coupled climate model. Journal of Geophysical Research 106, 2441–2464.

Blunier, T., Brook, E.J., 2001. Timing of millenial-scale climate change in Antarctica and Greenland during the last glacial period. Science 291, 109–112.

Blunier, T., Chappellaz, J., Schwander, J., Dällenbach, A., Stauffer, B., Stocker, T.F., Raynaud, D., Jouzel, J., Clausen, H.B., Hammer, C.U., Johnsen, S.J., 1998. Asyncrony of Antarctic and Greenland climate change during the last glacial period. Nature 394, 739–743.

Broecker, W.S., 1998. Paleocean circulation during the last deglaciation: a bipolar seesaw? Paleoceanography 13, 119–121.

Bryan, F., 1986. High-latitude salinity effects and interhemispheric thermohaline circulations. Nature 323, 301–304.

Caillon, N., Jouzel, J., Chappellaz, J., 2001. Reconstruction of the surface temperature change in central Greenland during D/O 12, 45 kyr b.p. In Eos Trans. AGU, volume 82.

Charles, C.D., Lynch-Stieglitz, J., Ninnemann, U.S., Fairbanks, R.G., 1996. Climate connections between the hemisphere revealed by deep sea sediment core/ice core correlations. Earth and Planetary Science Letters 142, 19–27.

Clark, P.U., Pisias, N.G., Stocker, T.F., Weaver, A.J., 2002. The role of the thermohaline circulation in abrupt climate change. Nature 415, 863–869.

Cox, M.D., 1989. An idealized model of the world ocean. Part I: the global-scale water masses. Journal of Physical Oceanography 19, 1730–1752.

Crowley, T.J., 1992. North Atlantic Deep Water cools the southern hemisphere. Paleoceanography 7, 489–497.

Cuffey, K.M., Clow, G.D., Alley, R.B., Stuiver, M., Waddington, E.D., Saltus, R.W., 1995. Large Arctic temperature change at the Wisconsin–Holocene glacial transition. Science 270, 455–458.

Ewen, T., Schmittner, A., Weaver, A.J., 2002. Modelling carbon cycle feedbacks during abrupt climate change, in preparation.

Fanning, A.F., Weaver, A.J., 1996. An atmospheric energy–moisture balance model: climatology, interpentadal climate change, and coupling to an oceanic general circulation model. Journal of Geophysical Research 110, 15,111–15,128.

Ganopolski, A., Rahmstorf, S., 2001. Stability and variability of the thermohaline circulation in the past and future: a study with a coupled model of intermediate complexity. In: Seidov, D., Haupt, B.J., Maslin, M.(Eds.), The Oceans and Rapid Climate Change. Past, Present and Future. Geophysical Monograph Series, Vol. 126, AGU, Washington, DC, pp. 261–275.

Gent, P.R., McWilliams, J.C., 1990. Isopycnal mixing in ocean circulation models. Journal of Physical Oceanography 20, 150–155.

Hastenrath, S., 1982. On meridional heat transports in the World Ocean. Journal of Physical Oceanography 12, 922–927.

Hinnov, L.A., Schulz, M., Yiou, P., 2002. Interhemispheric space–time attributes of the Dansgaard–Oeschger oscillations between 100 and 10 ka. Quaternary Science Reviews 21, 1213–1228.

Hsiung, J., 1985. Estimates of global oceanic meridional heat transport. Journal of Physical Oceanography 15, 1405–1413.

Indermühle, A., Monnin, E., Stauffer, B., Stocker, T.F., Wahlen, M., 2000. Atmospheric CO_2 concentrations from 60 to 20 kyr bp from the Taylor Dome ice core, Antarctica. Geophysical Research Letters 27, 735–738.

Johnsen, J., Dansgaard, W., White, J.W.C., 1989. The origin of Arctic precipitation under present and glacial conditions. Tellus 41B, 452–468.

Johnson, H.L., Marshall, D.P., 2002. A theory for the surface Atlantic response to thermohaline variability. Journal of Physical Oceanography 32, 1121–1132.

Jouzel, J., Alley, R.B., Cuffey, K.M., Dansgaard, W., Grootes, P., Hoffmann, G., Johnsen, S.J., Koster, R.D., Peel, D., Shuman, C.A., Stievenard, M., Stuiver, M., White, J., 1997. Validity of temperature reconstructions from water isotopes in ice cores. Journal of Geophysical Research 102, 26,471–26,487.

Maier-Reimer, E., Mikolajewicz, U., Crowley, T.J., 1990. Ocean general circulation model sensitivity experiment with an open central American isthmus. Paleoceanography 5, 349–366.

Manabe, S., Stouffer, R.J., 1988. Two stable equilibria of a coupled ocean–atmosphere model. Journal of Climate 1, 841–866.

Manabe, S., Stouffer, R.J., 1997. Coupled ocean–atmosphere model response to freshwater input: Comparison to Younger Dryas event. Paleoceanography 12, 321–336.

Manabe, S., Stouffer, R.J., 2000. Study of abrupt climate change by a coupled ocean-atmosphere model. Quaternary Science Reviews 19, 285–299.

Marchal, O., Stocker, T.F., Joos, F., Indermühle, A., Blunier, T., Tschumi, J., 1999. Modelling the concentration of atmospheric CO_2 during the Younger Dryas climate event. Climate Dynamics 15, 341–354.

Mikolajewicz, U., 1996. A meltwater-induced collapse of the 'conveyor belt' thermohaline circulation and its influence on the distribution of $\Delta^{14}C$ and $\delta^{18}O$ in the oceans. Technical Report 189, Max-Planck-Inst. für Meteorologie, Hamburg, Germany, pp. 1–25.

Mulvaney, R., Röthlisberger, R., Wolff, E.W., Sommer, S., Schwander, J., Hutterli, M.A., Jouzel, J., 2000. The transition from the last glacial period in inland and near-coastal Antarctica. Geophysical Research Letters 27, 2673–2676.

Pacanowski, R., 1995. MOM 2 documentation user's guide and reference manual, GFDL ocean group technical report. Technical Report, NOAA, GFDL, Princeton.

Peltier, W.R., 1994. Ice age paleotopography. Science 265, 195–201.

Rind, D., Russell, G., Schmidt, G., Sheth, S., Collins, D., deMemocal, P., Teller, J., 2001. Effects of glacial meltwater in the GISS coupled atmosphere–ocean model, 2. A bipolar seesaw in Atlantic Deep Water production. Journal Geophysical Research 106, 27, 355–27,365.

Rühlemann, C., Mulitza, S., Müller, P.J., Wefer, G., Zahn, R., 1999. Warming of the tropical Atlantic ocean and slowdown of thermohaline circulation during the last deglaciation. Nature 402, 511–514.

Salamatin, A.N., Lipenkov, V.Y., Barkov, N.I., Jouzel, J., Petit, J.R., Raynaud, D., 1998. Ice core age dating and paleotemperature calibration based on isotope and temperature profiles from deep boreholes at Vostok Station (East Antarctica). Journal Geophysical Research 103, 8963–8977.

Schiller, A., Mikolajewicz, U., Voss, R., 1997. The stability of the thermohaline circulation in a coupled ocean–atmosphere general circulation model. Climate Dynamics 13, 325–347.

Schmittner, A., Yoshimori, M., Weaver, A.J., 2002. Instability of glacial climate in a model of the ocean–atmosphere–cryosphere system. Science 295, 1493–1498.

Steig, E.J., Alley, R.B., 2002. Phase relationships between Antarctic and Greenland climate records. Annals of Glaciology, Vol. 35.

Steig, E.J., Brook, E.J., White, J.W.C., Sucher, C.M., Bender, M.L., Lehman, S.J., Morse, D.L., Waddington, E.D., Clow, G.D., 1998. Syncronous climate changes in Antarctica and the North Atlantic. Science 282, 92–95.

Stocker, T.F., 1998. The seesaw effect. Science 282, 61–62.

Stocker, T.F., 2000. Past and future reorganisations in the climate system. Quaternary Science Reviews 19, 301–319.

Stocker, T.F., Wright, D.G., Mysak, L.A., 1992. A zonally averaged, coupled ocean–atmosphere model for paleoclimate studies. Journal of Climate 5, 773–797.

Vellinga, M., Wood, R.A., Gregory, J.M., 2002. Processes governing the recovery of a perturbed thermohaline circulation in HadCM3. Journal of Climate 15, 764–780.

Weaver, A.J., Eby, M., Wiebe, E.C., Bitz, C.M., Duffy, P.B., Ewen, T.L., Fanning, A.F., Holland, M.M., MacFadyen, A., Matthews, H.D., Meissner, K.J., Saenko, O., Schmittner, A., Wang, H., Yoshimori, M., 2001. The UVic Earth System Climate Model: model description, climatology, and applications to past, present and future climates. Atmosphere-Ocean 39, 361–428.